PREPRINT

PERTANIKA JOURNALS

SCIENCE & TECHNOLOGY

Journal homepage: http://www.pertanika.upm.edu.my/

Characterisation of $BaFe_{12-2x}Cu_xNi_xO_{19}$ as Microwave Absorbing Materials on Radar Systems

Susilawati[1]*, Aris Doyan[1], Ali M. A. Abdul Amir Al-Mokaram[2], Mohammed Ahmed Ali Omer[3], Wan Yusmawati Wan Yusoff[4], Muhammad Taufik[1], Saprizal Hadisaputra[5], Yana Taryana[6], Nanang Sudrajat[7], Dedi Riyan Rizaldi[8], Ziadatul Fatimah[9], Muhammad Ikhsan[10], and Nuraini Rachma Ardianti[10]

[1]Physics Education, Faculty of Teacher Training and Education, University of Mataram, 83125, Indonesia
[2]Department of Chemistry, College of Science, Mustansiriyah University, Baghdad, 14022, Iraq
[3]Department of Radiologic Technology, College of Applied Medical Sciences, Qassim University, 51452 Buraidah, Saudi Arabia
[4]Physcis Department, Centre of Defense Foundation Studies, Universiti Pertahanan Nasional Malaysia, 57000 Kuala Lumpur, Malaysia
[5]Chemistry Education, Faculty of Teacher Training and Education, University of Mataram, 83125, Indonesia
[6]Research Centre for Telecommunication, Indonesian Institute of Sciences, 40116 Bandung, West Java, Indonesia
[7]Research Centre for Electronics, National Research and Innovation Agency, 10340 Jakarta, Indonesia
[8]Madrasah Aliyah Plus Nurul Islam Sekarbela, Mataram, 83116, Indonesia
[9]Senior High School Nahdlatul Wathan Mataram, Mataram, 83126, Indonesia
[10]Balai Publikasi Indonesia, Mataram, 83361, Indonesia

ABSTRACT

This research aims to test the characterisation of the barium ferrite copper nickel oxide ($BaFe_{12-2x}Cu_xNi_xO_{19}$) sample as a microwave absorbing material that will be applied to radio detection and ranging (Radar). The materials used in the synthesis process are barium carbonate ($BaCO_3$), iron oxide (Fe_3O_4), copper sulfate ($CuSO_4$), and nickel(II)chloride hexahydrate ($NiCl_2.6H_2O$) powders, while the solutions are 12 M hydrochloric acid (HCl), ammonium hydroxide (NH_4OH), and distilled water, which has been synthesised using the coprecipitation method with varying ion doping x = 0.0, 0.4, 0.8, and 1.0%, which is calcined at temperatures of 200, 600, and 1,000°C. The samples were then tested for characteristics through four stages of testing, namely X-ray diffraction (XRD), Fourier transform independent infrared spectroscopy (FTIR), transmission electron microscope (TEM), vibrating sample magnetometre (VSM),

ARTICLE INFO

Article history:
Received: 31 December 24
Accepted: 08 April 2025
Published: 20 January 2026

DOI: https://doi.org/10.47836/pjst.34.1.02

E-mail addresses:
susilawatihambali@unram.ac.id (Susilawati)
aris_doyan@unram.ac.id (Aris Doyan)
ali75@uomustansiriyah.edu.iq (Ali M. A. Abdul Amir Al-Mokaram)
ma.omer@qu.edu.sa (Mohammed Ahmed Ali Omer)
yusmawati@upnm.edu.my (Wan Yusmawati Wan Yusoff)
taufik@unram.ac.id (Muhammad Taufik)
rizal@unram.ac.id (Saprizal Hadisaputra)
yanaty73@gmail.com (Yana Taryana)
nana017@brin.go.id (Nanang Sudrajat)
dedi0313@gmail.com (Dedi Riyan Rizaldi)
ziadatulfatimah96@gmail.com (Ziadatul Fatimah)
muhammadikhsan99.mi@gmail.com (Muhammad Ikhsan)
nurainirachmaa@gmail.com (Nuraini Rachma Ardianti)
* Corresponding author

and vector network analyser (VNA). The test results using FTIR produced peaks at wave numbers 584-1639 cm^{-1}, which indicated the presence of Ba-O, Fe-O, Cu-O, and Ni-O functional groups. This indicates that the materials used in the synthesis process reacted or were present in the final sample. The test results using TEM with a sample of x = 1.0% and a calcination temperature of 1,000°C show that the resulting particles are hexagonal with a size of 50 nm. Tests using VSM show that the low coercivity value decreases, and the magnetic remanence and magnetic saturation values increase along with the use of ion doping and calcination temperature. The sample underwent a change from hard magnetic to soft magnetic based on the results of a decrease in the coercivity value and has the potential to become a microwave-absorbing material. The final test results using VNA produced a reflection loss value of -22.456 dB with an absorption percentage of 99.62%. The maximum electrical conductivity produced is 1.20305 σ at a temperature of 1,000°C. According to the indicators, the sample meets the criteria to be applied as a microwave-absorbing material, namely having a nanoparticle size, being soft magnetic, and being included as a semiconductor material.

Keywords: Barium M-hexaferrite (BaM), characterisation, doping, microwaves, radar system

INTRODUCTION

Indonesia itself has 17,380 islands, and of them, 111 small outer islands have been designated in the Presidential Decree No. 6 of 2017 concerning the Determination of Small Outer Islands, which need to be managed and secured. These islands are vulnerable or have the potential to become a source of conflict, so their existence needs to be maintained because it is a manifestation of state sovereignty. In this case, it is necessary to develop technology related to the use of electromagnetic waves, the use of which is currently developing very rapidly in various fields, including telecommunications, electronics, military, and civil. One of the most important parts in anticipating these conditions is developing a good defense or military system (Oxenham, 2010).

Radar, or radio detection and ranging, is a system that emits electromagnetic waves at a particular object and then receives and analyses its reflected waves to determine the position and distance of an object. In the field of military defense, radar has an important role as one of the systems that can help in the security control of the country's territory (Gustomo & Suwadi, 2013). Radar functions to detect the presence of other ships, weather conditions, or other objects around the ship (Kurniadi et al., 2023). The development of radar in the defense sector cannot be separated from improvements that have shortcomings, namely that the electromagnetic waves emitted will radiate in continuous waves. This causes radar to be able to detect the presence of an object, but not at the exact location. In 1936, with the development of pulsed radar, it is apparently able to interrupt the signal rhythmically, making it possible to determine the exact speed and direction of the target through the size of the inter-echoes (Zohuri, 2020). In the field of military defense, coating methods using radar-absorbing material (RAM) are used.

One of the technologies being developed in the military sector to eliminate enemy traces is called stealth technology. Engineering this technology by making the equipment invisible to the radar that is working (Fatimah et al., 2022). The engineering in making this stealth technology is by designing the corners of the aircraft and by coating the aircraft parts using RAM. RAM dampens reflection and absorbs microwaves (absorbers) so that materials coated with RAM cannot be detected by radar (David et al., 2022). The development of radar system technology research before and after World War II led to the interaction between electromagnetic wave radiation and materials. One aspect of the research is an effort to reduce or weaken the reflected signal from the radar (Taryana et al., 2019). Material used as an absorber must qualify, i.e., the material must have high permeability (μ), high permitivity (ε), low coercivity (Hc) field, and high magnetic saturation (Ms) (Pratitajati & Manaf, 2013). This is done not only to reduce radar signals through layers of absorbent materials on surrounding structures, such as radar support masts, towers, and supporting buildings, that can reduce the performance of the radar itself, but furthermore, the layer of material can also help weaken the reflected signal so that it is not detected by enemy radar.

The material used as an absorber is barium hexaferrite type M. Barium hexaferrite has been classified into six types based on its structure. The first is $BaFe_{12}O_{19}$ (type M), the second is $BaMe_2Fe_{16}O_{27}$ (type W), the third is $Ba_2Me_2Fe_{28}O_{46}$ (type X), the fourth is $Ba_2Me_2Fe_{12}O_{22}$ (type Y), the fifth is $Ba_3Me_2Fe_{24}O_{41}$ (type Z), and the last is $Ba_4Me_2Fe_{36}O_{60}$ (type U), where Me is the divalent ion of the first transition series or the symbol for a bivalent metal (having a charge of +2), such as cobalt (Co), nickel (Ni), or zinc (Zn), which partially replaces the iron in the hexaferrite structure (Ahmed et al., 2008). Due to the high magnetic power possessed by barium M-hexaferrite (BaM), its absorption properties will become weak, and it is necessary to adjust with other metal cations that have almost the same ionic radius as iron (Fe) ionic fingers. Ferrite magnets, in addition to having relatively high permeability, permittivity, and spontaneous magnetisation, are also composed of oxide components, so they also have high electrical resistivity or are good insulators (Priyono & Manaf, 2010). The combination of intrinsic properties between the magnetic and electrical properties of ferrite places ferrite magnetic materials as buffers for microwaves, including waves with frequencies used in radar. The advantages of barium hexaferrite include having a large magnetic crystalline anisotropy, high coercivity (6,700 Oe), a Curie temperature (450°C), relatively large saturation magnetisation (78 emu/g), good chemical stability, corrosion resistance, and being relatively easy to manufacture (Himanshi et al., 2023; Saidah & Zainuri, 2012; Tan & Chen, 2013).

Doping used is copper (Cu) and nickel (Ni) because it has almost the same ionic radius as Fe. It belongs to the transition group and has unpaired electrons. This is due to the more unpaired electrons, the stronger the magnetic properties of a material (Mott, 1936). Apart from that, the use of Cu and Ni is because both have high electrical and

thermal conductivity. Cu-Ni alloys are single-phase alloys in all compositions within the stage chart, and numerous standard alloys have specific phases and compositions within the stage graph (Nwaeju et al., 2021). This can be since Cu and Ni are totally miscible in both strong and fluid shapes. BaM with doping ions Cu and Ni written with the notation $BaFe_{12-2x}Cu_xNi_xO_{19}$.

Based on the description above, characterisation of $BaFe_{12-2x}Cu_xNi_xO_{19}$ was conducted using four tests, the first being FTIR. Second is TEM, third is VSM, and the fourth is VNA. The results of this characterisation are expected to have properties that are in accordance with microwave absorbent materials and provide an idea of whether the sample material from the results of characterisation that has been done can meet the criteria to be applied as a microwave absorbent material in radar systems.

MATERIALS AND METHODS

This study employs an experimental method that involves two stages: synthesis and characterisation. The synthesis process was carried out at the Basic Chemistry Laboratory, Faculty of Mathematics and Natural Sciences, University of Mataram. In the synthesis process, $BaFe_{12-2x}Cu_xN_ixO_{19}$ powder was produced. The powder was obtained from the basic materials of BaM and natural iron sand ($BaFe_{12}O_{19}$), which were modified with Cu and Ni metal ions that were dissolved with hydrochloric acid (HCl, Supelco®, Germany) and precipitated using ammonium hydroxide (NH_4OH, Supelco®, Germany) and neutralised with distilled water. The concentrations used were (x = 0, 0.4, 0.8, and 1.0%) The use of variations in concentration is carried out to obtain a calculated ratio of the precursors used in an even manner according to the reaction of each concentration which is then calcined with varying temperatures (200, 600, and 1,000°C) using the coprecipitation method (Prasetyowati et al., 2021). After obtaining the powder, the characterisation process was carried out in several laboratories, including. Characteristic tests using FTIR in the Analytical Chemistry Laboratory, FMIPA, UNRAM, which produces electromagnetic wave spectra to identify compounds contained in the sample and to determine the functional groups of the sample.

Characteristic tests using the TEM in the Analytical Chemistry Laboratory, FMIPA, UGM, which produce images and particle sizes of the sample to determine the structure and morphology of the sample. Characterisation test using XRD and VSM tool was done in Batan Puspitek Serpong Laboratory, which produces a hysteretic curve based on Hc, Ms, and Mr values to determine the magnetic properties of the sample. The last one is using a VNA in the Electronics and Telecommunication Research Centre Laboratory of the Indonesian Institute, which produces conductivity value data and reflection loss (RL) values, aiming to determine the electrical properties and microwave absorption ability. The achievement parameters used by the researcher are shown in Table 1.

Table 1
Measurement condition parameter

No.	Characteristic test	Measurement conditions
1	X-ray diffraction (XRD)	Detect crystal compounds in materials
2	Fourier transform infrared spectroscopy (FTIR)	Analyze the functional groups contained in the sample
3	Transmission electron microscope (TEM)	Produces images from the transmission of electrons through a sample in a vacuum chamber by knowing the particle size. Nanoparticles are particles between 1 and 100 nanometres in size
4	Vibrating sample magnetometre (VSM)	To measure the magnetic properties of materials where the Hc value on the graph narrows to near zero
5	Vector network analyser (VNA)	• To measure reflections at high frequencies, namely with the highest negative RL values • To measure the absorbance value of the sample • To measure the conductivity value of samples made from semiconductors

Note. Hc = Coercivity; RL = Reflection loss

RESULTS AND DISCUSSION

Based on the characterisation that has been done, the resulting data is as follows:

Testing using XRD

To characterise the sample crystals, XRD measurements were carried out on samples treated with different reaction times and temperatures. Testing using phase XRD aims to determine the crystal structure formed by the synthesised barium hexaferrite powder. XRD testing was carried out at the highest concentration and temperature, namely x = 1.0% and T = 1,000°C. This is because the sample is representative of knowing whether a crystal structure is formed. The test results using XRD can be seen in Figure 1.

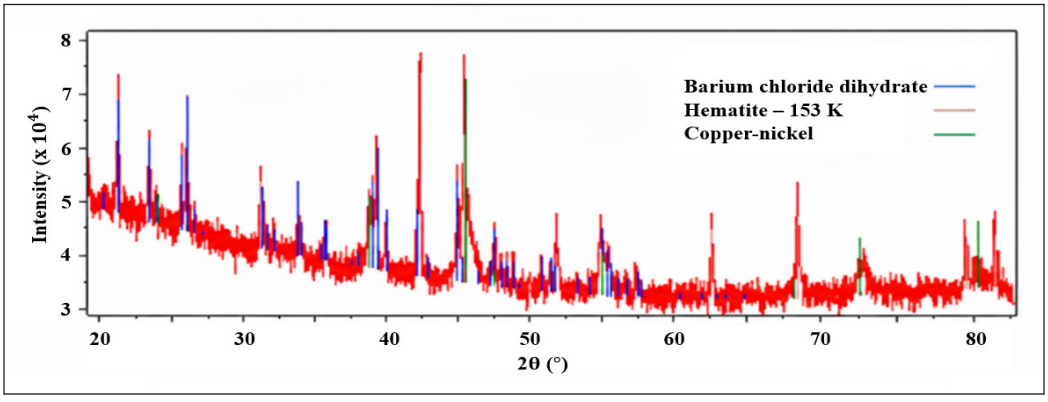

Figure 1. The graph of the relationship between the diffraction angle (2θ) and the diffraction X-ray spectrum (intensity) of barium M-hexaferrite powder doped with copper and nickel metal ions

The test was carried out at a voltage of 30 kV and a current of 20 mA using a Cu Kα target at a wavelength of λ = 1,532 A. Based on the graph above, the peak phase of barium hexaferrite at a diffraction angle of 2 is 26.4854°. The barium phase forms iron oxide, and manganese forms 45.704° iron oxide phase. Next, to test the crystal structure, the test results show that the lattice parameters a = b = 5.0471 Å and c = 12,739 Å, with angles α = β = γ = 80 and 110°. These results indicate that a hexagonal crystal structure has been formed.

Testing using FTIR

FTIR is one of the instruments that uses the principle of spectroscopy. Spectroscopy is an infrared spectroscopy equipped with a Fourier transform for the detection and analysis of spectral results. Infrared spectroscopy is useful for identifying organic compounds because of its very complex spectrum consisting of many peaks (Coates, 2006). In addition, each functional group absorbs infrared light at a unique frequency. The core of FTIR is the Michelson interferometre, a tool for analysing frequencies in combined signals. The infrared spectrum is produced from the transmission of light passing through the sample, measuring the light intensity with a detector, and comparing it with the intensity without the sample as a function of wavelength. The infrared spectrum obtained is then plotted as an intensity function of energy, wavelength (μm), or wave number (cm^{-1}).

Testing using FTIR produces a graph of the relationship between transmittance (%) and wave number (cm^{-1}) which shows the composition of the compounds contained in the sample by knowing the functional groups based on the wave number value using the highest concentration and temperature, namely x = 1.0% and T = 1,000°C. This is because the sample is representative in knowing whether there are functional groups made from BaM-O, Fe-O, with doping of Cu-O and Ni-O metal ions. The test results can be seen in Figure 2.

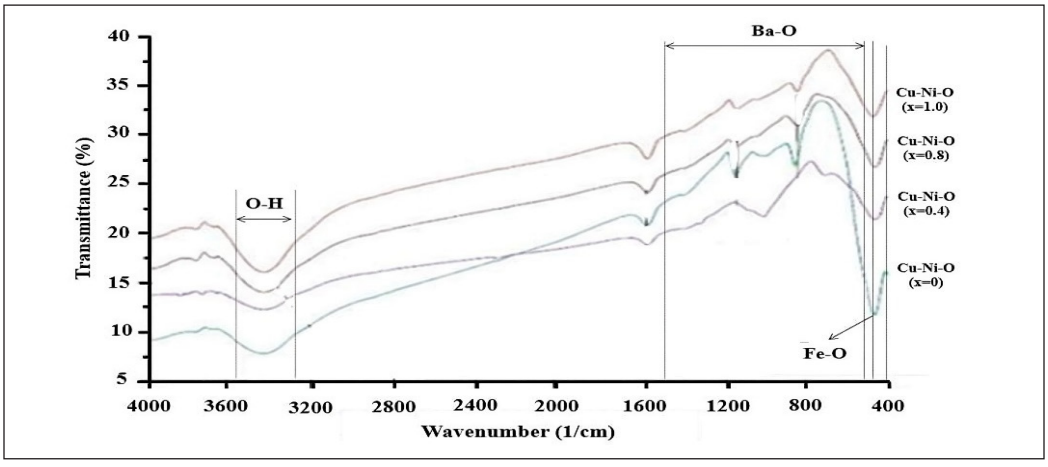

Figure 2. Test results using Fourier transform infrared spectroscopy at a calcination temperature of 1,000°C
Note. Ba-O = Barium oxide; O-H = Hydroxide; Cu-Ni-O = Copper nickel oxide; Fe-O = Iron oxide

Based on the graph in Figure 2, it appears that the presence of the barium phase M-hexaferrite is known based on the presence of stretching vibrations and bending between compounds characterised by differences in the resulting peak value. So, this sample can be said to form a BaM phase, which was successfully doped with Cu and Ni metal ions (Sözeri et al., 2016). This is proven by the presence of Cu-O and Ni-O bonds, which are at the peak of 449 cm^{-1}. This is in accordance with the range of metal ions as doping, namely Cu–O and Ni–O, namely the range of 400 to 663 cm^{-1} (Jang et al., 2013; Stuart, 2004). Meanwhile, the wave number of the BaM compound is at a peak of 1200 cm^{-1}, in accordance with the Ba–O range, namely in the range of 1000 to 1650 cm^{-1} (Doyan et al., 2015). It is characteristic of the metal bonds of oxygen that is characteristic of barium hexaferrite (Trukhanov et al., 2017).

Another visible metal bond is Fe-O at the peak of 542 cm^{-1}. The wave number is in accordance with the range of Fe-O, which is around 450 to 690 cm^{-1} (Doyan et al., 2017; Setiadi et al., 2016). These bonds indicate that there is a metal bond in the tested sample. The metal bonds are BaM, Fe, and Cu and Ni metal ions used as doping ($BaFe_{12-2x}Cu_xNi_xO_{19}$). So, it can be said that the process of making samples as RAM was successful, with the proof of the bond between BaM and Fe with Cu, Ni in the powder that has been produced.

Testing using TEM

TEM has a magnification of up to millions. In magnification on its objects, it has a resolution that is much better than a light microscope, where the electron microscope uses more energy and shorter electromagnetic radiation compared to a light microscope. The working principle of TEM is that the electron beam illuminates the sample and produces an image on the phosphor screen (Carter & Williams, 2016). In this study, the characteristic test using the TEM aims to determine the structure of the powder particles produced in the synthesis process, namely barium ferrite copper nickel oxide ($BaFe_{10}Cu_{1.0}Ni_{1.0}O_{19}$) at the highest temperature, namely 1,000°C.

Based on Figure 3, the test results show that the crystal size obtained is 100 nm, still large enough to carry out further measurements, and a crystal size of 50 nm is obtained. Nanoparticles are particles that are between 1 and 100 nanometres in size (Priyo, 2017). As material dimensions approach values of several nanometres, many physical and chemical properties become size dependent (Katsnelson et al., 2012; Tian, 2017). Typically, smaller grain sizes (nano order) produce higher active energies that influence magnetic saturation and field coercivity (Duan et al., 2018; Harahap & Nainggolan, 2022). This results in a wealth of properties and opportunities to manipulate or generate new ones that are not found in bulk materials.

Based on Figure 3, there is a component formed, namely a hexagon with a size of 50 nm. When compared with previous researchers who only got a size of 100 nm, it can

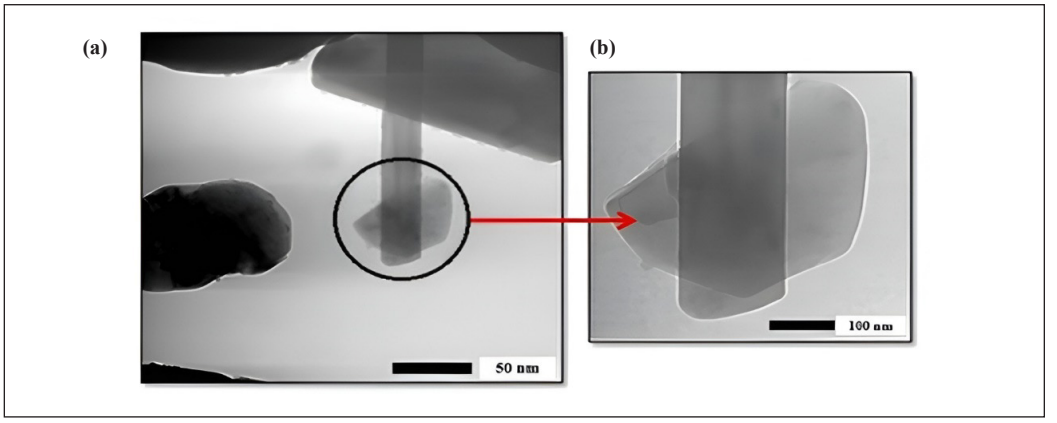

Figure 3. Transmission electron microscope test results: (a) indicates the particle size at a magnification of 50 nm; and (b) indicates the particle size at a magnification of 100 nm

be said that the BaM sample doped with Cu and Ni metal ions succeeded in getting a smaller crystal size in the nanometre range. This comparison is in accordance with research conducted by Nengsih (2018), Panduwinata et al. (2019), and Winatapura et al. (2013), which stated that the sample particle size can be stated as nanoparticles because in each study, a sample size of 100 nm was obtained and nano sized BaM samples have wide application opportunities (Asri et al., 2021).

Similarly, Ridwan and Winataputra (2018) found out the presence of hexaferrite particles through TEM testing by looking at the structure of smaller particles resembling hexagonal. Barium hexaferrite with a hexagonal structure ($BaFe_{12}O_{19}$) has been known as a permanent magnetic material that has high performance (Saidah & Zainuri, 2012).

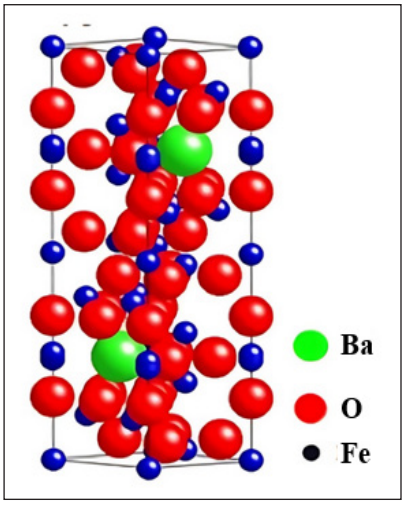

Figure 4. Perspective of the M-type barium hexaferrite ($BaFe_{12}O_{19}$) unit cell (Pullar, 2012)
Note. Ba = Barium; O = Oxygen; Fe = Iron

It can be seen in Figure 4 that BaM, with its hexagonal structure ($BaFe_{12}O_{19}$), is known as a permanent magnetic material that has high performance (Munib et al., 2016). This is in line with the opinion of Krichevtsov et al. (2024), which states that BaM is a permanent magnet with high magnetic anisotropy. The high crystal anisotropy of BaM so that it has a resonance frequency of around 50-60 Hz and is considered very high (Ghasemi, et. al., 2006). The crystal structure of BaM is hexagonal with lattice parameters a = b = 5.892 Å, c = 23.183 Å (Mallick, 2007). The BaM complex cell consists of 2 crystal systems, namely the face-centred-cubic and hexagonal-close-packed structures.

Testing using VSM

Characterisation of VSM is used to determine the magnitude of magnetic properties of materials in the form of Mr, Ms, and Hc (Ramadhan et al., 2018). Remanent magnetisation is the magnetic induction left in the material after the external magnetic field is removed. The coercivity field is the field required to remove remanent magnetisation. In comparison, saturation magnetisation is a condition where the magnetic spins in the material are in line with the external magnetic field (Nugraha et al., 2015).

The crystal structure factor has a very significant influence on the properties of permanent magnets. The Hc value is also influenced by the purity of the raw materials and the size of the crystal, which plays a role in inhibiting the movement of the domain walls. The smaller the crystal size, the more boundaries between crystals and the more barriers to the movement of the domain walls, so that the resistance to the demagnetisation field is greater, which means the Hc value is higher. Conversely, the larger the crystal size, the easier the domain walls move so that the resistance to the demagnetisation magnetic field is smaller, which means the Hc value is smaller.

VSM Test Results using Temperature Variations

Testing using VSM is to determine the magnetic properties of a material based on a hysteresis curve. The magnetic hysteresis curve is a characteristic curve of a magnetic material when given an external magnetic field and shows the relationship between the magnetisation value (Ms, Mr, and Hc) (Harahap & Sidabutar, 2020). The results of the VSM test are shown in Figure 5.

The hysterical curve in Figure 5, shows the change in the shape of the curve based on the Ms, Mr, and the Hc values obtained.

Based on the hysterical curve, it is seen that test samples with temperature variations at different concentrations of doping ions (0.0, 0.4, 0.8, and 1.0) indicate that the greater the calcination temperature used will produce the smaller the curve based on its Hc value, as the values of Mr and Ms will be smaller as the calcination temperature is used. The lowest Hc value is found at the concentration of doping ions x = 1.0%, calcined at a temperature of 1,000°C which is 0.025 T, as well as the value of Mr, which is 1.820 emu/g, and Ms, which is 3.980 emu/g. The value decreases due to the increase in calcination temperature, causing its magnetic properties to decrease. According to Sembiring et al. (2020), it was found that the mass density value increased with increasing temperature for all additive material compositions. This is understandable because volume usually increases because faster-moving molecules are further apart, which can affect the magnetic properties of the material. As can be seen from the graph, the higher the calcination temperature used, the higher the density of the material. Calcination itself aims to remove water content in the material so that the sample tested is the pure final mass obtained (Efhana & Zainuri, 2014).

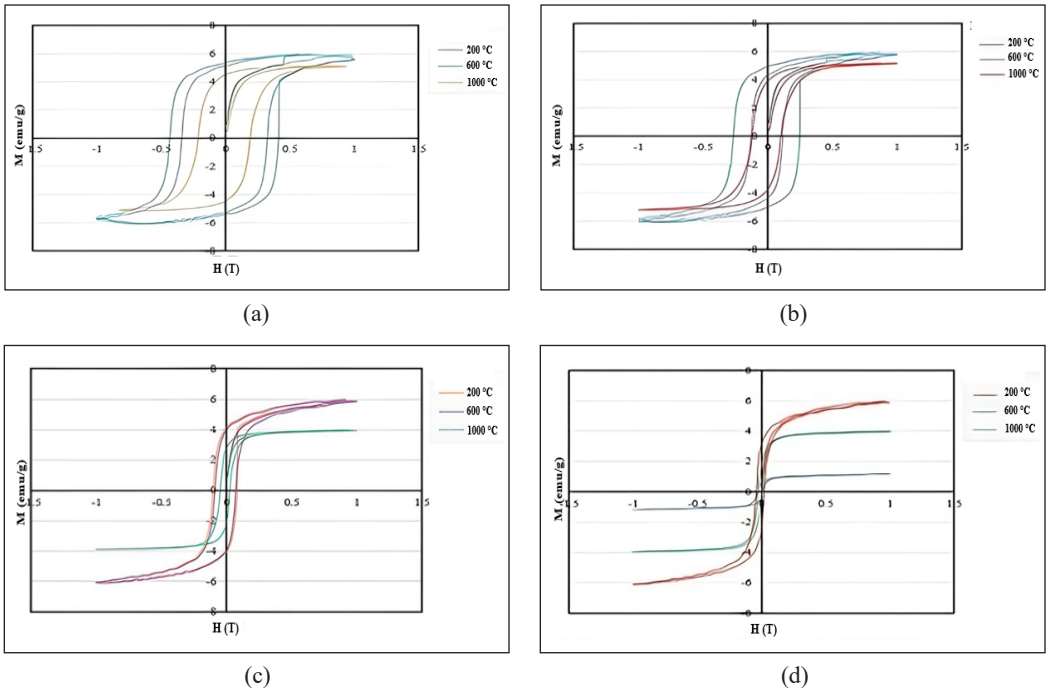

Figure 5. Hysteretic curves of temperature variations at 200, 600, and 1,000°C for samples with doping concentrations: (a) 0.0%; (b) 0.4%; (c) 0.8%; and (d) 1.0%
Note. M = Magnetisation; H = Magnetic field strength; T = Tesla

VSM Test Results using Variations in Doping Ions

In Figure 6, the data results obtained not only show the magnetic properties of the material but also show the influence of the doping and calcination temperature used, so that the characteristics of the magnetic hysteresis curve can be used to conclude whether the magnetic material is soft magnetic or still hard magnetic.

The hysterical curve of the test sample with a concentration of doping ions x = 0.0, 0.4, 0.8, and 1.0%, calcined at temperatures of 200, 600, and 1,000°C indicates curves with smaller shapes as doping ions are used, as well as the values of Hc, Mr, and Ms, which experienced a decrease.

The data obtained not only shows the magnetic properties of the material but also shows how much the metal ions as doping and the calcination temperature used so on the characteristics of the magnetic hysteresis curve, which can be used to conclude that the magnetic material is included in soft or hard magnetic (Susilawati et al., 2025). The magnetic properties of BaM in the sample show that the hysteresis curve increases with high magnetisation values (Ms and Mr) and Hc, in contrast to the doped sample, so that the magnetisation is greater (Ms and Mr) and the Hc is getting smaller. This causes the sample to become a soft magnetic material. These results are indicated by the presence of a hysteresis

curve when subjected to a magnetic field or when demagnetised. It can also be seen from the width of the hysteresis curve, which is getting narrower. This causes the material to become soft and magnetic.

The lowest Hc value is found at the concentration of doping ions x = 1.0%, calcined at a temperature of 1,000°C, which is 0.024 T, as well as the value of Mr, which is 1.816 emu/g, and Ms, which is 3.901 emu/g. The value decreased due to the increase in Cu and Ni doping ions, causing its magnetic properties to decrease. This is because in changing BaM, which was originally hard magnetic and will be changed into soft magnetic, engineering is needed according to the needs or what is desired. One of these engineering approaches is by taking an approach using plus ion substances, plus two, plus three, and more simultaneously, which aims to combine the positive properties of each doping component. A number of studies have been conducted to modify magnetic properties using plus two ions such as Co-Mn (Susilawati et al., 2017), Zn-Mn (Susilawati et al., 2019), and Mn-Ti (Widiyanto et al., 2011). The decrease in magnetism is very desirable because the BaM, which was originally hard magnetic, has turned into a soft magnetic. Changes in the properties of BaM from hard magnetic to soft magnetic based on the results of decreased coercivity values can potentially be a microwave absorbent material (Jia et al., 2018).

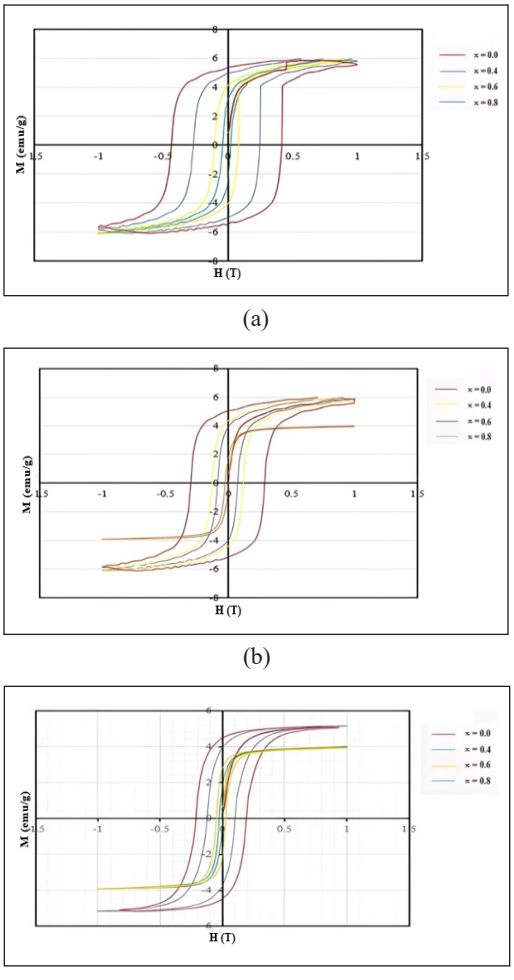

Figure 6. Hysteretic curves of concentration doping at x = 0.0, 0.4, 0.6, and 0.8% for samples with variations in temperature: (a) 200°C, (b) 600°C, and (c) 1,000°C

Note. M = Magnetisation; H = Magnetic field strength; T = Tesla

It can be said that there has been a magnetisation process caused by the increase in the external field, so that saturation and demagnetisation occur. Demagnetisation is the process of removing the external field. This is supported by research that has been conducted by Hedayatnasab et al. (2017), which states that the Hc value is inversely proportional to the Ms and Mr values, namely, when the Ms and Mr values increase, there is a decrease in

the Hc value approaching zero on the hysteresis curve graph. This is in accordance with the theory that the Hc value is obtained from demagnetisation with a certain value, so that magnetisation is zero, while saturation magnetisation is a condition obtained from an increase in the external field that occurs from the point of origin, so that saturation occurs. This saturation is due to having experienced a direction caused by an external magnetic field. From the saturation state and the coercive field with a value of zero, there is no return to the original curve shape, but there is a remaining magnetic flux. The remaining flux is called remanent magnetisation. In this state, the magnetic moment does not return to the orientation before being given an external field, which causes the material to be partially magnetized. So, samples substituted by Cu and Ni doping ions are said to decrease the anisotropic properties of BaM.

The magnetic properties of BaM in the $BaFe_{12}O_{19}$ sample show a wider hysteresis curve with large magnetisation values (Ms and Mr) and Hc, in contrast to the sample given doping, so that it experiences an increase in magnetisation (Ms and Mr) and a decrease in Hc, which makes the sample a soft magnetic material. The results are marked by the presence of a hysteresis curve when subjected to a magnetic field or when demagnetised and can be seen from the width of the hysteresis curve, which is getting narrower. Thus, it can be concluded that the sample with a concentration of x = 1.0% ($BaFe_{10}Cu_{1.0}Ni_{1.0}O_{19}$) has succeeded in reducing the magnetic properties of the material, which was initially without doping, namely $BaFe_{12}O_{19}$, which is still hard magnetic until using doping, so that it obtains soft magnetic properties and can be applied to microwave-absorbing materials.

Testing using VNA

VNA Test Results using Temperature Variations

VNA uses the concept of measuring transmitted and reflected waves as a signal passes through the device under test. Measuring the transmitted and reflected signals across the band of interest, and often beyond, allows the characteristics of the device to be determined (Pallás-Areny & Webster, 2012). If the transmitted and reflected signals are used to characterise the input as well as the output, then the device can be fully characterised. This can be a vital part of any design or testing of radio frequency (RF) circuits.

The test conducted using the VNA tool aims to determine the RL value, absorption, and conductivity. The RL value indicates the ability of a material to absorb microwaves; the percentage of absorption indicates that the amount of absorption power in the sample we synthesise indicates that the sample has the potential to be an absorbent material. While the conductivity value can indicate the electrical properties of the material, it can also indicate whether it is included in the semiconductor or not.

Graph of RL Values. BaM, which is known as ferric-magnetic, has stable chemical properties, is anti-corrosive, and has high anisotropy and is included in the hard magnet group, where, if its application wants to be efficient, it can be formed into a soft magnet. Magnets are soft magnetic materials that can be used as absorbers of microwaves. The hard magnetic properties of BaM are then engineered using metal-doping ions to reduce the hard magnetic properties to soft ones. This is in accordance with Yusnafi et al. (2017), who stated that BaM, which has the magnetic properties of a hard material, can be doped with more than one metal ion to get the properties of a soft magnet. So, it can be used as a microwave absorber material easily and economically. The requirement for the microwave absorbing material itself is to have a large negative RL value. The RL value shows the ability of a material to absorb microwaves (Soehada et al., 2018), where the greater the negative RL value produced, the greater the material's absorption of microwaves (Alam et al., 2015). The graph in Figure 7 is a graph of the relationship between frequency and RL value, producing values that vary based on the rise and fall of the RL value.

Based on Figure 7, a graph of RL values against frequencies with temperature variations of 200, 600, and 1,000°C at 0.0, 0.4, 0.8, and 1.0%, which results in a greater RL value as the calcination temperature is increased. The greater the negative RL value, the greater

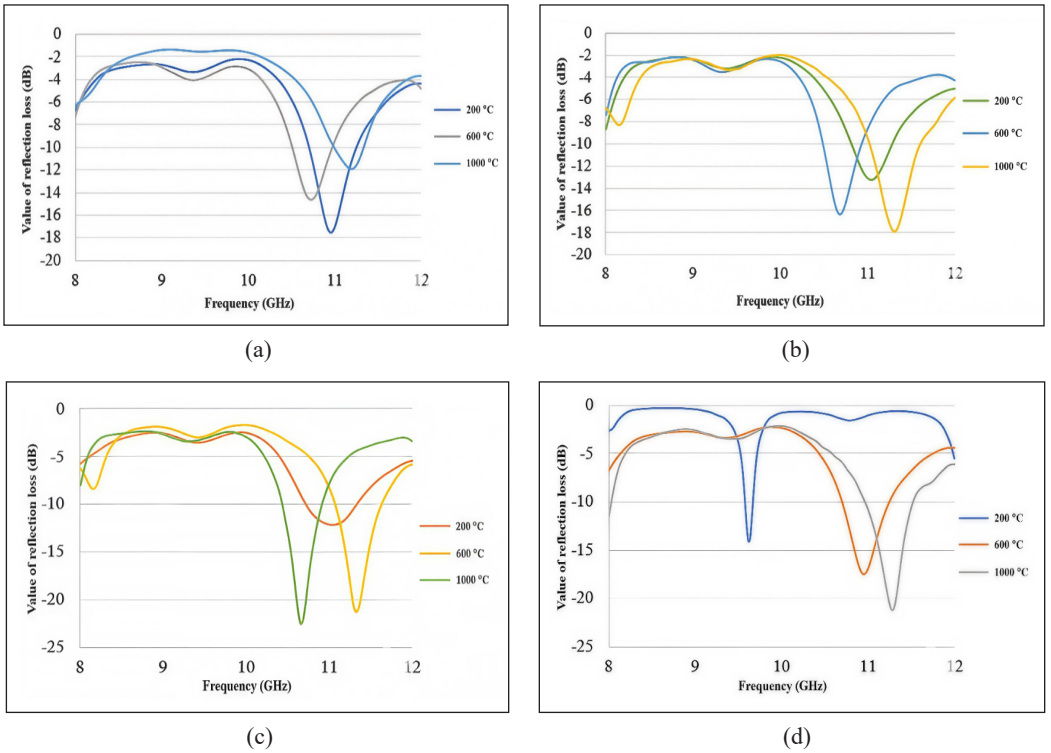

Figure 7. Reflection loss value graph of temperature variations at 200, 600, and 1,000°C for samples with doping concentrations: (a) 0.0%, (b) 0.4%, (c) 0.8%, and (d) 1.0%

the absorption result and the smaller the reflection. The number of doping ions and the high calcination temperature used can affect the RL value in the sample. As seen in Figure 7, the maximum RL value at a concentration of x = 1.0 with a calcination temperature of 1,000°C of -22.456 dB. The RL value and absorption coefficient greatly affect the absorption power of microwaves produced by the sample. The greater the RL value produced, the higher the absorption percentage. The maximum absorption percentage obtained was 99.62%, which shows that the sample powder has the potential to be a microwave-absorbing material (Susilawati et al., 2019). Basically, good absorption of electromagnetic waves is characterised by a low reflection value and has a wide absorption band or large frequency interval because it can absorb microstructures in various frequency ranges (Wulandari et al., 2024).

Graph of Conductivity Values. Electrical conductivity is a measure of a material's ability to conduct an electric current. Figure 8 shows a graph of the relationship between frequency and conductivity value.

For Figure 8, the graph of the value of electrical conductivity to frequencies with temperature variations that produce the lowest conductivity value of 0.12006 σ is found at 600°C and the highest temperature of 1.20305 σ is found at 1,000°C and is included in the semiconductor category.

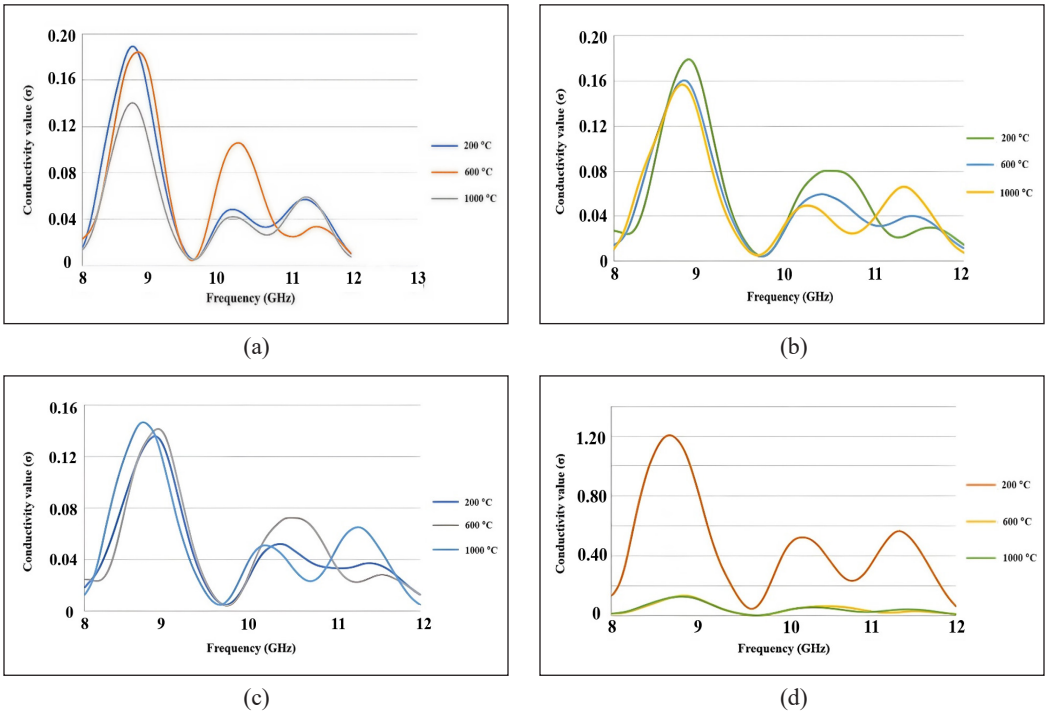

Figure 8. Graph of conductivity values of temperature variations at 200, 600, and 1,000°C for samples with doping concentrations: (a) 0.0%, (b) 0.4%, (c) 0.8%, and (d) 1.0%

Good electrical conductors have a conductivity value of 10^7 σ, while insulating materials have very low conductivity values, namely between 10^{-10} σ and 10^{-20} σ. Between these two properties, semiconductor materials have conductivity values of 10^{-7} to 10^3 σ (Mahmood et al., 2015). Based on the results obtained, it can be concluded that the sample is very good for use as an energy absorber. The formation of an electric field on the absorber surface occurs when microwaves hit the material coated with microwave absorber material, after which a current flows as a surface current so that it can convert microwaves into heat energy microwaves because the semiconductor material can convert microwave energy into heat energy.

VNA Test Results using Variations in Doping Ions

Graph of RL Values. Based on Figure 9, the graph of the value of RL against frequency with variations in doping ions is 0.0; 0.4; 0.8; and 1.0% at 200, 600, and 1,000°C temperatures, resulting in greater RL values as the doping ion is used, the maximum RL value produced is -18.3282 dB in the sample x = 1.0% and with a calcination temperature of 1,000°C. The higher the concentration used, the percentage of metal ions as doping will also increase, which results in a large negative RL value in the sample, as indicated by the nature of the sample, namely soft magnetic, which has been tested using a VSM tool.

This is because the RL value and absorption coefficient greatly affect the microwave absorption power produced by the sample. The greater the RL value produced, the higher the absorption percentage (Yunasfi et al., 2017). The requirements that must be met in the manufacture of microwave-absorbing materials are that the material used must have a high conductivity value, because it is good for use as an absorbing material.

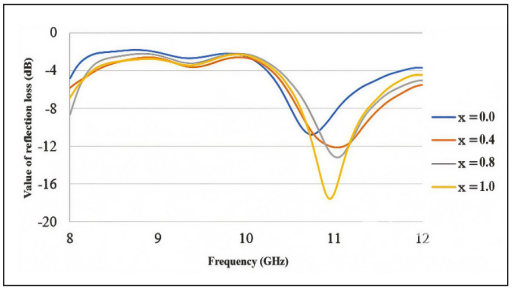

(a)

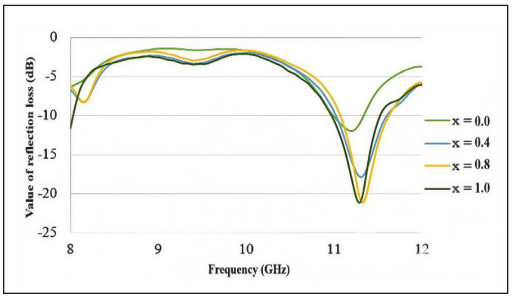

(b)

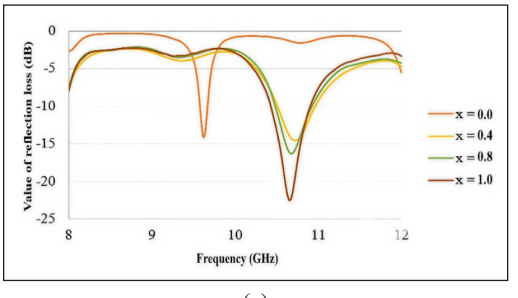

(c)

Figure 9. Reflection loss value graph of concentration doping at x = 0.0, 0.4, 0.6, and 0.8% for samples with variations temperature: (a) 200°C, (b) 600°C, and (c) 1,000°C

Graph of Conductivity Values. In Figure 10, the graph of electrical conductivity values against frequency with variations in doping ion concentration produces the lowest conductivity value of 0.12471 σ at a temperature of 1,000°C and the highest of 1.18448 σ at a temperature of 200°C, and is included in the semiconductor category. Concentration influences the effect of concentration on measuring the conductivity of materials, sometimes different from other tests. If the concentration used is high, the percentage of material used is also large according to the calculation. So that at the highest concentration, namely the metal ions used, are much more, which produces a significant reaction than other samples. This is in accordance with previous research, namely the formation of an electric field on the absorber surface, namely when microwaves hit the material coated with microwave absorbent material, where after that the current flows as a surface current so that it can convert microwaves into heat energy. The results of this study are supported by research conducted by Fithriyani (2017), which obtained a conductivity value of 1.62 × 10^{-2} σ and is classified as a semiconductor material.

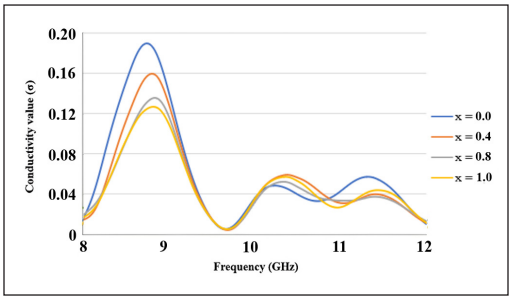

(a)

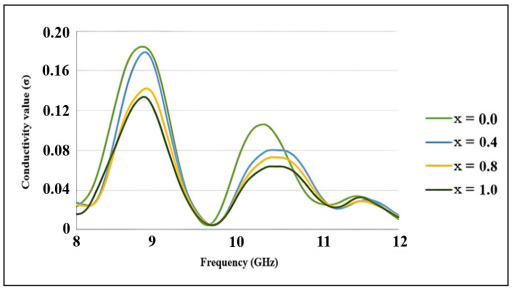

(b)

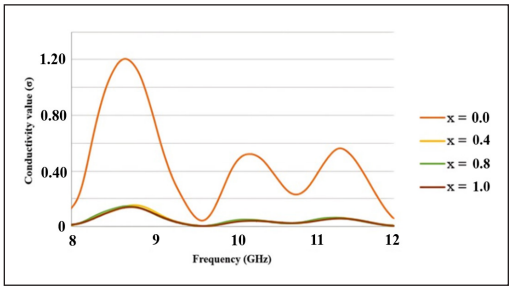

(c)

Figure 10. Conductivity value graph of concentration doping at x = 0.0, 0.4, 0.6, and 0.8% for samples with variations temperature: (a) 200°C, (b) 600°C, and (c) 1,000°C

CONCLUSION

Based on the results and discussion of the characterisation tests that have been carried out, it can be concluded that testing has been successfully carried out on $BaFe_{12-2x}Cu_xNi_xO_{19}$ powder with the final result being that at a concentration of x = 1.0 and a temperature variation of T = 1,000°C producing peaks at certain wave numbers in accordance with the wave number characteristics of each peak (Ba-O = 1.200 cm^{-1}, Fe-O = 542 cm^{-1}, and Co-O, Ni-O = 449 cm^{-1}) with a particle size of 50 nm in the sample, so it is included in the nanoparticles. Some components have been formed, namely, hexagonal. For the

magnetic properties of the sample, the Hc, Mr, and Ms values are directly proportional to the concentration at each temperature. It can be said that the $BaFe_{12-2x}Cu_xNi_xO_{19}$ sample is included in the soft magnetic properties and is in accordance with theory 1.0%. T = 1,000℃ can also be used as a microwave absorbing material because it is included in the semiconductor material, namely the conductivity value is 1.20305 σ with the highest RL, namely -22.456 dB, which produces an absorption value of 99.62% so that the sample (mole fraction (x) = 1.0%) with a temperature variation of T = 1,000℃ can be used as a microwave absorbing material with a high absorption capacity.

ACKNOWLEDGEMENT

This research was supported by a grant from the Public Service Agency Budget Implementation List of Overseas Research Cooperation Schemes, Universitas Mataram, for Fiscal Year 2025, under grant number 2491/UN18.I.1/PP/2025.

REFERENCES

Ahmed, M. A., Okasha, N., & Kershi, R. M. (2008). Influence of rare-earth ions on the structure and magnetic properties of barium W-type hexaferrite. *Journal of Magnetism and Magnetic Materials*, *320*(6), 1146-1150. https://doi.org/10.1016/j.jmmm.2007.11.014

Alam, R. S., Moradi, M., Rostami, M., Nikmanesh, H., Moayedi, R., & Bai, Y. (2015). Structural, magnetic and microwave absorption properties of doped Ba-hexaferrite nanoparticles synthesised by co-precipitation method. *Journal of Magnetism and Magnetic Materials*, *381*, 1-9. https://doi.org/10.1016/j.jmmm.2014.12.059

Asri, L., Didik, L. A., & Bahtiar, B. (2021). Sintesis dan analisis kandungan mineral dan karakteristik sifat listrik nanopartikel pasir besi Pantai Telindung Kabupaten Lombok Timur [Synthesis and analysis of mineral content and electrical properties of iron sand nanoparticles from Terlindung Beach, East Lombok Regency]. *Jurnal Sains dan Teknologi*, *10*(1), 85-91. https://doi.org/10.23887/jstundiksha.v10i1.22765

Carter, C. B., & Williams, D. B. (Eds.). (2016). *Transmission electron microscopy: Diffraction, imaging, and spectrometry* (1st ed.). Springer. https://doi.org/10.1007/978-3-319-26651-0

Coates, J. (2006). Interpretation of infrared spectra, a practical approach. In R. A. Meyers & M. L. McKelvy (Eds.), *Encyclopedia of analytical chemistry: Applications, theory and instrumentation* (pp. 10815-10837). John Wiley & Sons Ltd. https://doi.org/10.1002/9780470027318.a5606

David, D. A., Naiker, V., Fatima, J. M. J., George, T., Dhawale, P. V., Supekar, M. V., Begum, P. M. S., Thakur, V. J., & Raghavan, P. (2022). Polymer composites for stealth technology. In A. Srinivasan, S. Murugesan, & A. R. Mahendran (Eds.), *Progress in polymer research for biomedical, energy and specialty applications* (1st ed., pp. 383-420). CRC Press. https://doi.org/10.1201/9781003200710-18

Doyan, A., Halik, I., & Susilawati, S. (2015). Pengaruh variasi temperatur kalsinasi terhadap barium M-heksaferit didoping Zn menggunakan Fourier Transform Infrared [The effect of calcination temperature variations on Zn-doped barium M-hexaferrite using fourier transform infrared]. *Jurnal Pijar Mipa*, *10*(1), 7-13. https://doi.org/10.29303/jpm.v10i1.9

Doyan, A., Khalilurrahman, K., & Susilawati, S. (2017). Sintesis dan uji FTIR barium M-hexaferrite dengan doping logam Mn [Synthesis and FTIR test of barium M-hexaferrite with Mn metal doping]. *Jurnal Pendidikan Fisika dan Teknologi*, *1*(4), 235-238. https://doi.org/10.29303/jpft.v1i4.264

Duan, M., Shapter, J. G., Qi, W., Yang, S., & Gao, G. (2018). Recent progress in magnetic nanoparticles: Synthesis, properties, and applications. *Nanotechnology*, *29*(45), 452001. https://doi.org/10.1088/1361-6528/aadcec

Efhana, D. P., & Zainuri, M. (2014). Pengaruh Variasi Waktu Penahanan Proses Kalsinasi Terhadap Prekursor Bahan Katoda Lithium Ferrophospate (LFP). *Jurnal Sains dan Seni ITS*, *3*(2), B118-B122. https://www.neliti.com/publications/15461/pengaruh-variasi-waktu-penahanan-proses-kalsinasi-terhadap-prekursor-bahan-katod

Fatimah, Z., Susilawati., & Doyan, A. (2022). The process of making BaM ($BaFe_{12}O_{19}$) samples based on natural iron sand doped with metal (Co-Cu-Zn) using the coprecipitation method. In *Journal of Physics: Conference Series* (Vol. 2165, No. 1, p. 012007). IOP Publishing. https://doi.org/10.1088/1742-6596/2165/1/012007

Fithriyani, A. (2017). *Sintesis $BaFe_{12-2x}Zn_xMn_xO_{19}$ berbasis pasir besi alam dan pengujian struktur, sifat listrik dan magnet sebagai bahan penyerap gelombang mikro* [Synthesis of $BaFe_{12-2x}Zn_xMn_xO_{19}$ based on natural iron sand and analysis of its structural, electrical and magnetic properties as a microwave absorbing material] [Doctoral dissertation, Universitas Mataram]. Universitas Mataram Repository. https://eprints.unram.ac.id/2970/

Ghasemi, A., Hossienpour, A., Morisako, A., Saatchi, A., & Salehi, M. (2006). Electromagnetic properties and microwave absorbing characteristics of doped barium hexaferrite. *Journal of Magnetism and Magnetic Materials*, *302*(2), 429-435. https://doi.org/10.1016/j.jmmm.2005.10.006

Gustomo, F., & Suwadi, S. (2013). Analisa penggunaan sinyal radar bentuk pulsa dan gelombang kontinyu untuk target bergerak dengan model clutter terdistribusi Rayleigh [Analysis of the use of pulse and continuous wave radar signals with the Rayleigh distributed clutter model]. *Jurnal Teknik ITS*, *2*(2), A235-A240.

Harahap, V., & Sidabutar, S. (2020). Sintesis dan sifat magnetik komposit $BaFe_{12}O_{19}$/ZnO terhadap aplikasi elektronik media perekam dan absorben [Synthesis and magnetic properties of $BaFe_{12}O_{19}$/ZnO composites for applications in electronic recording and absorbent media]. *2-TRIK: Tunas-Tunas Riset Kesehatan*, *10*(2), 86-92.

Harahap, V., & Nainggolan, A. B. D. (2022). Coating radiation waves based on $BaFe_{12}O_{19}$/ZnO from natural red sand on X-ray radiation exposure in the Laboratory of Efarina Hospital in the era of the COVID-19 pandemic. *Journal of Aceh Physics Society*, *11*(1), 17-23. https://doi.org/10.24815/jacps.v11i1.21871

Hedayatnasab, Z., Abnisa, F., & Wan Daud, W. M. A. (2017). Review on magnetic nanoparticles for magnetic nanofluid hyperthermia application. *Materials and Design*, *123*, 174-196. https://doi.org/10.1016/j.matdes.2017.03.036

Himanshi., Jasrotia, R., Prakash, J., Verma, R., Thakur, P., Kandwal, A., Wan, F., & Thakur, A. (2023). Synthesis, characterisation, and applications of doped barium hexaferrites: A review. *Physica B: Condensed Matter*, *667*, 415202. https://doi.org/10.1016/j.physb.2023.415202

Jang, H. T., Jung, E. M., Park, S. H., & Hemalatha, P. (2013). Synthesis and characterisation of CoO-ZnO catalyst system for selective CO oxidation. *International Journal of Control and Automation*, *8*(6), 31-40. https://doi.org/10.14257/ijca.2013.6.6.04

Jia, Z., Lan, D., Lin, K., Qin, M., Kou, K., Wu, G., & Wu, H. (2018). Progress in low-frequency microwave absorbing materials. *Journal of Materials Science: Materials in Electronics*, *29*, 17122-17136. https://doi.org/10.1007/s10854-018-9909-z

Katsnelson, B. A., Privalova, L. I., Sutunkova, M. P., Khodos, M. Y., Shur, V. Y., Shishkina, E. V., Tulakina, L. G., Pichugova, S. V., & Beikin, J. B. (2012). Uptake of some metallic nanoparticles by, and their impact on pulmonary macrophages *in vivo* as viewed by optical, atomic force, and transmission electron microscopy. *Journal of Nanomedicine and Nanotechnology*, *3*(1), 1000129. https://doi.org/10.4172/2157-7439.1000129

Krichevtsov, B., Korovin, A., Fedorov, V., Suturin, S., Levin, A. A., Telegin, A., Balashova, E., & Sokolov, N. (2024). Thin films of BaM hexaferrite with an inclined orientation of the easy magnetisation axis: Crystal structure and magnetic properties. *Nanomaterials*, *14*(23), 1883. https://doi.org/10.3390/nano14231883

Kurniadi, D., Sahputra, A., & Arifin, Z. (2023). Optimalisasi penggunaan radar: Kompetensi operator radar, perencanaan pemasangan radar dan spesifikasi radar [Optimizing radars use: Radar operator competence, radar installation planning and radar specifications]. *Journal of Engineering and Transportation*, *1*(1), 1-9.

Mahmood, S. H., Aloqaily, A. N., Maswadeh, Y., Awadallah, A., Bsoul, I., Awawdeh, M., & Juwhari, H. (2015). Effects of heat treatment on the phase evolution, structural, and magnetic properties of Mo-Zn doped M-type hexaferrites. *Solid State Phenomena*, *232*, 65-92. https://doi.org/10.4028/www.scientific.net/SSP.232.65

Mallick, K. K., Shepherd, P., & Green, R. J. (2007). Dielectric properties of M-type barium hexaferrite prepared by co-precipitation. *Journal of the European Ceramic Society*, *27*(4), 2045-2052. https://doi.org/10.1016/j.jeurceramsoc.2006.05.098

Mott, N. F. (1936). The electrical conductivity of transition metals. *Proceedings of the Royal Society A: Mathematical and Physical Sciences*, *153*(880), 699-717. https://doi.org/10.1098/rspa.1936.0031

Munib., Susilawati., & Savalas, L. R. T. (2016). Sintesis barium M-hexaferritte ($BaFe_{12-x}Ni_xO_{19}$) doping logam nikel dengan metode kopresipitasi [Synthesis of barium M-hexaferrite ($BaFe_{12-x}Ni_xO_{19}$) doped with nickel metal by coprecipitation method]. *Jurnal Penelitian Pendidikan IPA*, *2*(1), 9-17. https://doi.org/10.29303/jppipa.v2i1.28

Nengsih, S. (2018). Potensi nanopartikel magnetit pasir besi Lampanah Aceh Besar melalui studi kajian teknik pengolahan, sintesis dan karakteristik struktur [The potential of magnetite nanoparticles in Lampanah iron sand, Aceh Besar, through studies of processing techniques, synthesis, and structural characteristics]. *CIRCUIT: Jurnal Ilmiah Pendidikan Teknik Elektro*, *2*(1). https://doi.org/10.22373/crc.v2i1.3246

Nugraha, P. R., Widanarto, W., Cahyanto, W. T., & Kuncoro, H. S. (2015). Pengaruh aditif $BaCO_3$ pada kristalinitas dan suseptibilitas barium ferit dengan metoda metalurgi serbuk isotropic [Effect of $BaCO_3$ additive on crystallinity and susceptibility of barium ferrite using isotropic powder metallurgy method]. *Berkala Fisika*, *18*(1), 43-50.

Nwaeju, C. C., Edoziuno, F. O., Adediran, A. A., Nnuka, E. E., & Adesina, O. S. (2021). Structural and properties evolution of copper-nickel (Cu-Ni) alloys: A review of the effects of alloying materials. *Matériaux and Techniques*, *109*(2), 204. https://doi.org/10.1051/mattech/2021022

Oxenham, D. (2010). The next great challenges in systems thinking: A defence perspective. *Civil Engineering and Environmental Systems*, *27*(3), 231-241. https://doi.org/10.1080/10286608.2010.482661

Pallás-Areny, R., & Webster, J. G. (2012). *Sensors and signal conditioning*. John Wiley & Sons, Inc.

Panduwinata, F., Mahmudin, L., & Iqbal, I. (2019). Fabrikasi dan karakterisasi sifat optik nanopartikel magnetit Fe_3O_4 berbasis pasir besi [Fabrication and characterisation of optical properties of iron sand based Fe_3O_4 magnetite nanoparticles]. *Gravitasi*, *18*(1), 1-10. https://doi.org/10.22487/gravitasi.v18i1.13296

Prasetyowati, R., Widiawati, D., Swastika, P. E., Ariswan, A., & Warsono, W. (2021). Sintesis dan karakterisasi nanopartikel magnetit (Fe_3O_4) berbasis pasir besi Pantai Glagah Kulon Progo dengan metode kopresipitasi pada berbagai variasi konsentrasi NH_4OH [Synthesis and characterisation of magnetite nanoparticles (Fe_3O_4) based on iron sand from Glagah Beach, Kulon Progo, using the coprecipitation method at various NH_4OH concentrations]. *Jurnal Sains Dasar*, *10*(2), 57-61. https://doi.org/10.21831/jsd.v10i2.43043

Pratitajati, E., & Manaf, A. (2013). Microstructural characterisation and microwave absorption characteristics of $La_{(1-x)}Ba_xFe_{0.25}Mn_{0.5}Ti_{0.25}O_3$ (x= 0, 0.25, 0.75, 1). *Advanced Materials Research*, *789*, 161-166. https://doi.org/10.4028/www.scientific.net/AMR.789.161

Priyo, W. (2017). Manfaat nanopartikel di bidang kesehatan [Benefits of nanoparticles in the health sector]. *Majalah Farmasetika*, *2*(4), 1-3. https://doi.org/10.24198/farmasetika.v2i4.15891

Priyono., & Manaf, A. (2010). Material magnetic barium heksaferit tipe-M untuk material anti radar pada frekuensi *S-band* [M-type barium hexaferrite magnetic material for anti-radar materials at *S-band* frequency]. *Indonesian Journal of Materials Science*, *11*(2), 75-78.

Pullar, R. C. (2012). Hexagonal ferrites: A review of the synthesis, properties, and applications of hexaferrite ceramics. *Progress in Materials Science*, *57*(7), 1191-1334. https://doi.org/10.1016/j.pmatsci.2012.04.001

Ramadhan, M. I., Widanarto, W., & Sunardi, S. (2018). Pengaruh temperatur sintering terhadap struktur dan sifat magnetik Ni^{2+}-barium ferit sebagai penyerap gelombang mikro [The effect of sintering temperature on the structure and magnetic properties of Ni^{2+}-barium ferrite as a microwave absorber]. *Jurnal Teras Fisika: Teori, Modeling, dan Aplikasi Fisika*, *1*(1), 23-28. https://doi.org/10.20884/1.jtf.2018.1.1.567

Ridwan., & Winatapura, D. S. (2018). Karakterisasi stronsium heksaferit koersivitas tinggi hasil sintesis dengan metode kopresipitasi [Characterisation of high coercivity strontium hexaferrite synthesised by coprecipitation method]. *Jurnal Sains Materi Indonesia*, *13*(2), 141-145.

Saidah, I. N., & Zainuri, M. (2012). Pengaruh variasi pH pelarut HCl pada sintesis barium M-Heksaferrit dengan doping Zn ($BaFe_{11,4}Zn_{0,6}O_{19}$) menggunakan metode kopresipitasi [The effect of variations in the pH of HCl solvent on the synthesis of barium M-hexaferrite with Zn doping ($BaFe_{11,4}Zn_{0,6}O_{19}$) using coprecipitation method]. *Jurnal Sains dan Seni ITS*, *1*(1), B41-B46.

Sembiring, T., Sasniati, P., Muljadi., Sinuhaji, P., & Sebayang, K. (2020, March). Study of physical and magnetic properties of barium hexaferrite substituted by Nd_2O_3. In *AIP Conference Proceedings* (Vol. 2221, No. 1, p. 110025). AIP Publishing. https://doi.org/10.1063/5.0005256

Setiadi, E. A., Sebayang, P., Ginting, M., Sari, A. Y., Kurniawan, C., Saragih, C. S., & Simamora, P. (2016). The synthesization of Fe_3O_4 magnetic nanoparticles based on natural iron sand by co-precipitation method for the used of the adsorption of Cu and Pb ions. In *Journal of Physics: Conference Series* (Vol. 776, No. 1, p. 012020). IOP Publishing. https://doi.org/10.1088/1742-6596/776/1/012020

Soehada, A. M., Sebayang, K., Sudiro, T., Kurniawan, C., & Sebayang, P. (2018). Effect of Mn-Ti ions doping and sintering temperature on properties of barium hexaferrite. *Jurnal Sains Materi Indonesia*, *15*(4), 192-195.

Sözeri, H., Mehmedi, Z., Erdemi, H., Baykal, A., Topal, U., & Aktaş, B. (2016). Microwave properties of $BaFe_{11}Mg^{2+}_{0.25}X^{2+}_{0.25}Ti^{4+}_{0.25}O_{19}$ (X^{2+} = Cu, Mn, Zn, Ni and Co) nanoparticles in 0-26.5 GHz range. *Ceramics International*, *42*(2), 2611-2625. https://doi.org/10.1016/j.ceramint.2015.10.065

Stuart, B. H. (2004). *Infrared spectroscopy: Fundamentals and applications*. John Wiley & Sons. https://doi.org/10.1002/0470011149

Susilawati, S., Doyan, A., & S. Sahlam (2017). Synthesis and characterisation materials M-barium hexaferrite doping ions Co-Mn nano particle. In *IOP Conference Series: Materials Science and Engineering* (Vol. 196, No. 1, p. 012016). IOP Publishing. https://doi.org/10.1088/1757-899X/196/1/012016

Susilawati., Doyan, A., Al-Mokaram, A. M. A. A., Ali Omer, M. A., Taufik, M., Hadisaputra, S., Taryana, Y., Sudrajat, N., Rizaldi, D. R., Fatimah, Z., Ikhsan, M., & Ardianti, N. R. (2025). Characterisation $BaFe_{12-3x}Co_xCu_xZn_xO_{19}$ samples based on natural iron sand on electrical and magnetic properties as a microwave absorbent material. *Journal of Advanced Research in Micro and Nano Engineering*, *28*(1), 80-94. https://doi.org/10.37934/armne.28.1.8094

Susilawati., Doyan, A., Taufik, M., Wahyudi., Gunawan, E. R., Fitriani, A., & Nazarudin, N. (2019). Characterisation of barium M-hexaferrite with doping Zn and Mn for microwaves absorbent. *Materials Science Forum*, *966*, 282-289. https://doi.org/10.4028/www.scientific.net/MSF.966.282

Tan, G., & Chen, X. (2013). Structure and multiferroic properties of barium hexaferrite ceramics. *Journal of Magnetism and Magnetic Materials*, *327*, 87-90. https://doi.org/10.1016/j.jmmm.2012.09.047

Taryana, Y., Manaf, A., Sudrajat, N., & Wahyu, Y. (2019). Material penyerap gelombang elektromagnetik jangkauan frekuensi radar [Electromagnetic wave absorbing materials on radar frequency range]. *Jurnal Keramik dan Gelas Indonesia*, *28*(1), 1-28.

Tian, L. (2017). A short review on mechanical behavior of nanocrystalline materials. *International Journal of Metallurgy and Metal Physics*, *2*, 008.

Trukhanov, S. V., Trukhanov, A. V., Kostishyn, V. G., Panina, L. V., Turchenko, V. A., Kazakevich, I. S., Trukhanov, A. V., Trukhanov, E. L., Natarov, V. O., & Balagurov, A. M. (2017). Thermal evolution of exchange interactions in lightly doped barium hexaferrites. *Journal of Magnetism and Magnetic Materials*, *426*, 554-562. https://doi.org/10.1016/j.jmmm.2016.10.151

Widiyanto, W., Priyono, P., & Nurhasanah, I. (2011). Evaluasi perubahan struktur akibat substitusi parsial ion Mn^{2+} dan ion Ti Pada M heksaferit BaFe 12-2X Mn menggunakan analisis Rietveld [Evaluation of structural changes due to partial substitution of Mn^{2+} and Ti ions in BaFe 12-2X Mn hexaferrite using Rietveld analysis]. *BERKALA FISIKA*, *14*(3), 81-86.

Winatapura, D. S., Sukirman, E., Siti, W., & Purnama, S. (2013). Karakterisasi $BaFe_{12}O_{19}$ koersivitas tinggi hasil sintesis dengan metode kopresipitasi kimia [Characterisation of high coercivity $BaFe_{12}O_{19}$ synthesise chemical co-precipitation method]. *Jurnal Sains dan Teknologi Nuklir Indonesia*, *14*(2), 79-88.

Wulandari, F. P., Nur, A. A., Gafira, C. E., & Aritonang, S. (2024). Review jurnal: Nanokomposit sebagai penyerap gelombang elektromagnetik untuk radar *absorbent material* [Journal review: Nanocomposites as electromagnetic wave absorbers for radar absorbent materials]. *Jurnal Rekayasa Material, Manufaktur dan Energi*, *7*(1), 151-159.

Yunasfi., Masahdi., & Mulyawan, A. (2017). Sintesis bahan absorber gelombang mikro $Ni_{(1,5-x)}La_xFe_{1,5}O_4$ dengan metode sol gel [Synthesis of microwave absorber material $Ni_{(1,5-x)}La_xFe_{1,5}O_4$ using sol-gel method]. *Jurnal Sains Materi Indonesia*, *19*(1), 19-24.

Zohuri, B. (2020). *Radar energy warfare and the challenges of stealth technology*. Springer. https://doi.org/10.1007/978-3-030-40619-6